

Available online at www.sciencedirect.com

SciVerse ScienceDirect

journal homepage: www.intl.elsevierhealth.com/journals/jden

Color reproduction for advanced manufacture of soft tissue prostheses

Kaida Xiao^{a,*}, Faraedon Zardawi^{a,b}, Richard van Noort^a, Julian M. Yates^c

^a Academic Unit of Restorative Dentistry, School of Clinical Dentistry, University of Sheffield, Claremont Crescent, Sheffield S10 2TA, UK

^b Department of Periodontology, School of Dentistry, University of Sulaimani, Zanko Street, Iraq

^c Department of Oral & Maxillofacial Surgery, School of Dentistry, University of Manchester, Coupland III Building, Coupland Street, M13 9PL, UK

ARTICLE INFO

Article history:

Received 27 November 2012

Received in revised form

31 January 2013

Accepted 17 April 2013

Keywords:

Color reproduction

Soft tissue prostheses

Advanced manufacture

3D color printing

ABSTRACT

Objectives: The objectives of this study were to develop a color reproduction system in advanced manufacture technology for accurate and automatic processing of soft tissue prostheses.

Methods: The manufacturing protocol was defined to effectively and consistently produce soft tissue prostheses using a 3D printing system. Within this protocol printer color profiles were developed using a number of mathematical models for the proposed 3D color printing system based on 240 training colors. On this basis, the color reproduction system was established and their system errors including accuracy of color reproduction, performance of color repeatability and color gamut were evaluated using 14 known human skin shades. **Results:** The printer color profile developed using the third-order polynomial regression based on least-square fitting provided the best model performance. The results demonstrated that by using the proposed color reproduction system, 14 different skin colors could be reproduced and excellent color reproduction performance achieved. Evaluation of the system's color repeatability revealed a demonstrable system error and this highlighted the need for regular evaluation. The color gamut for the proposed 3D printing system was simulated and it was demonstrated that the vast majority of skin colors can be reproduced with the exception of extreme dark or light skin color shades.

Conclusions: This study demonstrated that the proposed color reproduction system can be effectively used to reproduce a range of human skin colors for application in advanced manufacture of soft tissue prostheses.

© 2013 Elsevier Ltd. All rights reserved.

1. Introduction

Every year thousands of patients require customised soft tissue prostheses to replace eyes, ears, noses, digits and other body parts affected by congenital defects, disease, surgery or trauma. Currently these are made from silicone polymers

using the traditional skills of maxillofacial technologists or anaplastologists.¹ The manufacture of these soft tissue prostheses is a lengthy and technically demanding process, and the outcomes are heavily dependent upon the skill of a small number of highly experienced technologists. For patients the process is often complicated, inconvenient and disconcerting.²

* Corresponding author at: School of Clinical Dentistry, University of Sheffield, 19 Claremont Crescent, Sheffield S10 2TA, UK. Tel.: +44 0114 271 7890; fax: +44 0114 279 7050.

E-mail address: k.xiao@sheffield.ac.uk (K. Xiao).

0300-5712/\$ – see front matter © 2013 Elsevier Ltd. All rights reserved.

<http://dx.doi.org/10.1016/j.jdent.2013.04.008>

An accurate color match between the subject's skin and the prosthesis is always highly desirable. Conventionally, color matching is achieved by subjectively assessing the patient's skin color and then reproducing that color by manually mixing color pigments into silicone polymer.³ As a consequence, even with significant levels of expertise it can be extremely difficult to achieve a sufficiently accurate match and often, fine adjustments/additions are needed in the later stages of production.

Recent advances in 3D digital imaging technology have enabled direct interconnectivity with advanced manufacturing techniques, and opened up the possibility of producing custom-based production models that offer excellent accuracy and savings in terms of both time and cost.⁴ This technique has been utilised for some time in the form of rapid prototyping and is now gaining popularity in non-manufacturing fields including medicine and dentistry.⁵ More recently, the use of 3D imaging production techniques in human skin reproduction for facial prosthetics has been recognised as an important innovative manufacturing process that may have a significant impact on the delivery of these prostheses to patients.⁶

However, the accuracy and consistency of color reproduction has become a critical element in the 3D advanced manufacture of soft tissue prostheses, and the current system still has significant shortcomings in this respect. This is primarily due to the RGB color systems used in the 3D color printing process being quite different from those deriving from human visual perception. That is to say, RGB color signals used in manufacturing processes cannot be directly linked to the processes within the human visual system, and in order to reproduce a subject's skin color that can be considered "accurate" in terms of human visual perception, a new color reproduction system has to be developed for the 3D color printing process.

Color management techniques developed over recent years play an important role in the translation of accurate color reproduction through different media.⁷ For instance, a color image on a digital screen can be accurately reproduced on paper (or other 2D printed surface) by conducting appropriate color management techniques for the display and printer. Compared with a conventional 2D color image, 3D images have larger image data and geometric factors to consider, and therefore are more complicated to process. Furthermore, 3D imaging devices are also more difficult to control and characterise, and thus conventional color management techniques cannot be applied directly to 3D imaging/manufacturing devices.

The primary objective of this study was to develop a color reproduction system for 3D color printing and to comprehensively evaluate its color reproduction performance and its application to the automated production of soft tissue prostheses. This new approach was based on the application of conventional color management techniques to a Zcorp 3D color printer. A specific color profile was established for the 3D color printing system to allow color transformation from any target LAB values to printer RGB values. The 3D color reproduction system was evaluated in terms of accuracy of color reproduction, performance of color repeatability and system color gamut.

2. Materials and methods

2.1. Protocol for 3D color printing

In this project, the primary focus was to consistently reproduce human skin tones using a 3D color printing system. A Zcorp Z510 3D color printer (Fig. 1) was employed and a protocol to produce soft tissue prostheses was developed and is described below.

Firstly, a 3D color image was sent to the 3D color printer for the printing of a 3D object using starch powder (Z15e, 3DSYSTEMS Limited). A resolution of 0.5 mm was selected to generate a medium range of thickness of each layer. During printing, printer heads released colored inks and a binder onto the powder foundation according to the prescribed layers within the 3D digital images. This allowed printing in a cross sectional 2D layer. The process was then repeated to produce a new 2D layer on top of the previous layer. The process of printing continues until a full 3D color object has been built up. In the second step, the 3D colored object was removed after printing within 20 min of completion and any excess powder removed. It was then left for 30 min in an airtight storage container. Next, infiltration processing was conducted in order to infiltrate the 3D object with a clear medical grade silicone polymer (Silskin 25). Previously it was determined that 1.4 mm infiltration can be achieved from each side of a 3D sample, thus indicating that the 3D sample can be fully infiltrated up to a thickness of 2.8–3.0 mm. Finally, the 3D object is left for 24 h to completely dry and allow the silicone to set.

2.2. Color measurement

In this study, a Minolta CM-2600d spectrophotometer using SpectraMagic NX Color Data Software was employed to take color measurements in CIELAB values.⁸ The illuminant was set to CIE standard D65 to simulate skin color in daylight conditions.⁸ During the measurement, a viewing geometry of $d/8$ (diffuse illumination, 8° viewing) was used, with the specular component included and the aperture size set to 3 mm. The instrument provides a consistent (repeatability $\leq 0.04\Delta E_{ab}^*$)⁸ and reliable color measurement (inter instrument agreement $< 0.2\Delta E_{ab}^*$).



Fig. 1 – Experimental set up for Zcorp Z510 printer.

2.3. Development of color profile for 3D printer

In order to accurately reproduce color data using the specific 3D color printer, a printer color profile was developed to directly link the printer color processing to human visual perception. More specifically, it enabled identified printer RGB data, specific to the target skin color, to be defined as CIELAB values. CIELAB values are well acknowledged as the universal standard basis of color specification and measurement. Furthermore, they are based on human visual perception and are independent of any imaging devices. To undertake this task, a specific color profile was developed in order to connect device independent CIE LAB values to device dependent printer RGB values. The device dependent color profiling produced represents a mathematical model that can calculate the relationship of color responses between the human eye and specific color device. In this study, one relatively straightforward method of developing a color profile was to record a number of different training color samples in terms of both device RGB values and CIE LAB values. Once undertaken, standardised modelling techniques were employed, including three-dimensional lookup tables with interpolation,⁹ least-squares polynomial regression^{10,11} or neural networks,¹² to derive a transformation between the CIE LAB Tristimulus values and device dependent RGB values. However, methods based on 3D lookup tables or neural networks require a large number of reference samples and only achieve a reasonable performance. Thus they are considered impractical for many digital applications, including the use of viewing equipment such as monitors and microscopes. In contrast, polynomial regression based on the least-squares method has been widely employed for developing camera and printer profiles and this is due to its accurate results and ease of implementation.¹³ Therefore, the latter was adopted to drive the 3D color printer profile in this study.

During these investigations, 240 colors from a digital Macbeth color chart were employed as training colors and their RGB values extracted in Adobe Photoshop. CIELAB values were then obtained by converting the 2D color chart to a 3D model with dimensions of 200 mm (l) × 150 mm (w) × 3 mm (h) printed by the Zcorp Z510 printer following the printing protocol described above. CIELAB values for each color patch in the printed color chart were then measured using the spectrophotometer. Following evaluation of the CIELAB values and corresponding printer RGB values for the 240 training colors, the relationship between the two was investigated using polynomial regression based on least-squares fitting. In order to place the two data sets within the same numeric scale, both sets of data were converted. CIELAB values were transformed to CIE XYZ Tristimulus values, RGB values divided by 255 and CIE XYZ Tristimulus values divided by 95, 100 and 108 in order for normalisation to CIE D65 standard light source to be undertaken.

For the polynomial regressions based on least-squares fitting, we referred to the original dataset as vectors [a b c] and these were mapped onto a target dataset (represented by vector p[x y z]) and N = number of training colors used in the color profiling process. For the original dataset (s_i for i = 1..N) formed an N × 3 matrix – O, and their target dataset (p_i for i = 1..N) forms N by means of 3 matrix – T. For the purpose of

linear mapping, the following objective function minimises the sum of squared residuals:

$$E = \sum_{i=1}^N (p_i^T - s_i^T M)^2 \tag{1}$$

where M is unknown, a transfer matrix was sought. Taking partial derivatives with respect to the elements of M, one arrives at the Euler equation:

$$O^T(T - OM) = 0 \tag{2}$$

Therefore, a least-squares solution is:

$$M = (O^T O)^{-1} O^T T \tag{3}$$

where O^T denotes the transposition of O, and O⁻¹ represents the inverse of O. The idea underpinning this simple linear transformation was that each column of T can be written as a linear combination of the columns of O. Therefore:

$$T = \alpha O_1 + \beta O_2 + \gamma O_3 \tag{4}$$

where α, β and γ are scalars. However, as a simple linear transformation often does not produce adequate results, the procedure was extended to higher-order polynomial terms to produce a more accurate model. Thus, in a second-order polynomial function, each column of T was represented not only as a linear combination of columns of O, but also of O squared (O₁², O₂², O₃²). Moreover, cross-column and translational terms were also be added into the function so that the N × 3 matrix O was expanded to the N × 11 matrix O^T:

$$O^T = [O_1 \ O_2 \ O_3 \ O_1^2 \ O_2^2 \ O_3^2 \ O_1O_2 \ O_1O_3 \ O_2O_3 \ 1] \tag{5}$$

where 1 denotes the N × 1 vector with all N components equal to 1 and accounts for translations. Similarly, a third-order polynomial function consisting of 20 terms listed in Eq. (6) was also investigated,

$$O^T = \begin{bmatrix} O_1 & O_2 & O_3 & O_1^2 & O_2^2 & O_3^2 & O_1O_2 & O_1O_3 & O_2O_3 & 1 & \dots \\ O_1^3 & O_2^3 & O_3^3 & O_1^2O_2 & O_1^2O_3 & O_2^2O_1 & O_2^2O_3 & O_3^2O_1 & O_3^2O_2 & \dots & \dots \end{bmatrix} \tag{6}$$

In theory it is acknowledged that there is no limit to the order and number of terms of the polynomial. However, in practice it is constrained by or limited to the accuracy required, the computational cost and the number of samples available. In this particular study, second and third order polynomial regression (Eqs. (5) and (6)) and a direct 3 × 3 matrix were used to evaluate the relationship, where CIE XYZ Tristimulus values were original matrices (O) and printer RGB target matrices were represented by T. The method with least predicted error between original printer RGB and model predicted RGB for the 240 training data was adopted for developing within our printer color profile.

2.4. 3D imaging reproduction system for human skin

The 3D color image reproduction system developed for soft tissue prostheses was based on two steps. The first step was to generate a 2D image from LAB values to printer RGB values for each color pixel using the proposed printer color profile. The

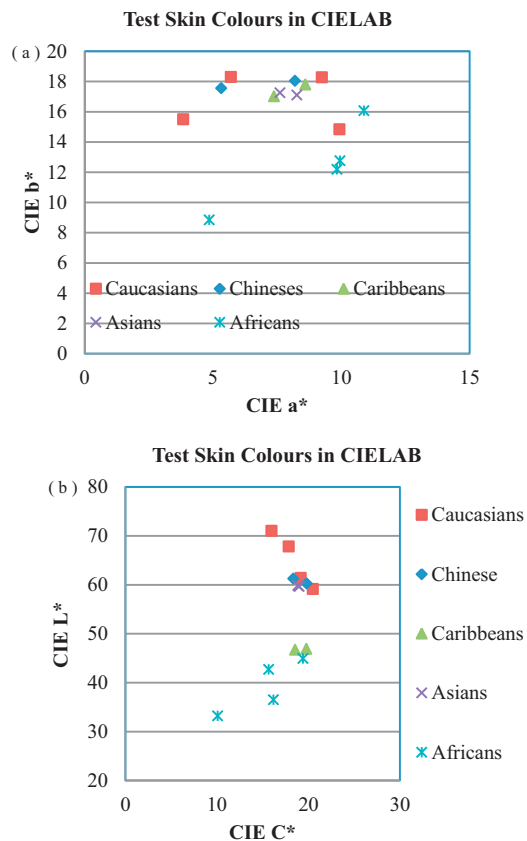


Fig. 2 – Distribution of test colors in CIELAB.

second step was to map the newly generated 2D image profile into the target 3D model for printing. This was undertaken using color texture mapping within the 3Matic software (Materialise Leuven, Belgium).

As the primary objective of this project was to focus on accurate production of skin tones, 14 known human skin colors including 4 Caucasian, 2 Chinese, 2 Asian, 4 African and 2 Caribbean skin shades, were used to evaluate the proposed color reproduction system. Their CIELAB values were obtained by direct skin color measurements using the Minolta CM-2600d spectrophotometer for 14 different subjects from 4 different ethnic groups utilising the skin on their cheek.¹⁴ Their color distributions in CIELAB color space were plotted in Fig. 2a and b. It can be seen that among these 14 testing colors, skin tones of the different ethnic groups were easily distinguishable.

These LAB values were referred to as the original LAB values. They were then transformed to CIE XYZ Tristimulus values and the corresponding printer RGB values using the proposed color reproduction system. These colors were then mapped onto a 3D chart with dimensions of 200 mm (l) × 150 mm (w) × 3 mm (h) and printed using the Zcorp Z510 color printer and following the proposed protocol. The spectrophotometer was then used to measure LAB values for each color patch – these were referred to as reproduced LAB values. Subsequently, the color reproduction performance was represented by the CIELAB color difference between the

original LAB values and reproduced LAB values for each skin color patch.

2.5. System color repeatability

Printer color repeatability represents the potential stability and consistency of color printing and was considered a significant problem within this manufacturing process. In this study it was evaluated by analysing the color shift produced when using the same printed color samples within a defined time interval – the 14 skin shades adopted previously as test colors and 1 non-colored shade were employed. Using the exact same settings and processes 10 identical 3D color chart were generated within a 20 day time period. The first color chart was considered the reference chart with all subsequent color charts regarded as testing color charts. Every color patch on each chart was measured using the spectrophotometer in terms of CIE LAB values. Any color changes within the 20 day time period, represented by the average color difference between the respective tones on the reference and testing color charts, were calculated.

2.6. System color gamut

The color gamut of the 3D printing system represents its color capability and directly affects the color reproduction performance. The 3D printer's potential color output determines what colors can be reproduced and ideally these need to be identified in order to determine whether the printer can encompass the color gamut of human skin. Based on the proposed color reproduction system, the 3D printer color gamut was predicted in CIELAB uniform color space using Segment Maximum GBD.¹⁵ This was undertaken to segment the color space specified gamut boundary value in terms of a two dimensional look-up-table. The gamut boundary was then generated in two dimensional lightness-chroma space with any known hue value. On this basis, the 3D model to represent the printer's color gamut was developed in CIELAB uniform color space using a VRML 2.0 visualisation package.¹⁶ Colors can only be reproduced by the proposed 3D printing system if they are within the boundaries of the 3D printer gamut.

2.7. Statistical analysis

In this study, the color data were objectively measured and compared in CIELAB uniform color space, where the color reproduction performance and color repeatability was measured by CIE ΔE_{ab}^* (Eq. (7)) and lightness, chroma and hue attributes were calculated for the color gamut. CIELAB uniform color space was uniform in each of its three directions of color, L^* , a^* and b^* – L^* represents lightness attributes in the range of 0–100 whilst a^* and b^* represents red–green and yellow–blue opponents. The latter are used to indicate color redness and color yellowness for human skin colors. From a^* and b^* values, C_{ab}^* and h values can be calculated to determine chroma and hue attributes. Chroma refers to representation of the perceived color intensity in terms of degree of difference between a color and grey with a

larger chroma value representing greater color intensity. Hue definition within a range of 0–360° indicates colors in red, green, blue, and yellow.

A distinct advantage of the CIE LAB color space is the simplicity of calculating a difference between two colors using the following equation:

$$\Delta E_{ab}^* = \sqrt{\Delta L^2 + \Delta a^2 + \Delta b^2} \tag{7}$$

where ΔL^* , Δa^* and Δb^* denote respective differences in the L^* , a^* and b^* color parameters between two colors.

Color difference unit (ΔE_{ab}^*) represents a uniform scale of color difference. All values are positive and a higher value represents a greater color difference. Means and standard deviations for a range of skin colors were calculated to assess the overall performance of the skin color reproduction system.

R^2 , the coefficient of determination, was adopted to indicate how well a mathematical model fitted a set of training data when the printer color profile was developed. R , the correlation coefficient, was employed in assessing whether each individual color attribute of a testing color affected system repeatability error.

3. Results

A color reproduction system was developed for the advanced manufacture of soft tissue prostheses using 3D printing and its performance in color reproduction evaluated using a range of known human skin tones. Furthermore, its color capability and repeatability, indicating the consistency of color gamut and color output respectively, was evaluated.

3.1. Printer color profile

For the 240 training color dataset, the performance of each mathematical transformation was evaluated in terms of the model's predicted error between original printer RGB and predicted printer RGB. The results on mean difference and standard deviation for each model are given in Table 1.

From these figures it can be seen that the third order polynomial regression model gave the best performance, whereas the linear transform performed significantly worse when compared to all the polynomial regressions. They all demonstrate a non-linear relationship between CIE XYZ and printer RGB for the specific 3D color printer used. To illustrate this the training data (represented by empty dots) and fitted 3rd order polynomial regression model (represented by a solid line) in each color channel were plotted, as shown in Fig. 3. It can be seen from Fig. 3 that each model indicates a good relationship for the training data used.

Table 1 – Model performance for training dataset.

RGB difference	Mean	STDEV
Linear transform	102.8	75.3
Second order polynomial	12.9	8.2
Third order polynomial	10.8	7.7

3.2. Performance of skin color reproduction

To evaluate the accuracy of the proposed 3D color reproduction system, the color difference between original LAB values and reproduced LAB values were calculated for 14 known skin colors. The results in terms of mean, maximum, minimum and standard deviation are shown in Table 2. Fig. 4 also illustrates the color reproduction performance for each skin shade. For soft tissue prostheses, color differences less than 3.0 units have been deemed acceptable, according to research published by Paravina et al.¹⁷ A solid black line was plotted in Fig. 4 to demonstrate the acceptable color difference when referring to skin color reproduction. This demonstrates that apart from one Caucasian skin color, the color reproduction error for the majority of skin tones was very close to $3\Delta E_{ab}^*$, indicating that color reproduction was acceptable.

By comparison, conventional inkjet printers, using the same approach, can achieve a color reproduction accuracy of approximately $2\Delta E_{ab}^*$.¹⁸ Therefore, our study indicates that the proposed color reproduction system cannot achieve the same level of performance with the 3D color printer. One of the main reasons for this is that the 3D color printing system cannot maintain a consistent color output due to its complicated processing method. Furthermore, when the color reproduction system was evaluated, the repeatability error affected the overall performance because the printer color profile was developed on the basis of the previous training chart and the evaluation was conducted for the subsequent printed testing color chart. Color repeatability is therefore a very important aspect of a color reproduction system and needs to be carefully evaluated.

3.3. Performance of color repeatability

The printer color repeatability was evaluated using 10 consecutive color charts printed within a 20 day period. The average color differences between the reference color chart and each test color chart were calculated for the 14 color shades and 1 non-colored shade respectively, and the results are given in Table 3. It can be seen that the color difference relating to the printer color repeatability is between 2 and $5\Delta E_{ab}^*$ for the color shades and 0 and 3 for the non-colored shade. These results demonstrate that significant color shifts occur when the same chart is printed at different time points. The average repeatability errors within the 20 day period were 3.0 and 1.7 for the color shades and non-colored shade respectively, which indicates that 43% of the repeatability error was generated by the printers color binder whilst the other 57% could have been generated during processing, for instance, in the starch powder, de-powdering or infiltration processes.

In order to illustrate the repeatability performance with time interval, Fig. 5 was plotted. The repeatability for the color shades is represented by the solid line, while the repeatability for non-colored shade is represented by the dashed line. It can be seen that the best repeatability/performance was achieved within 13 days and the worst performance was obtained at 20 days. In order to investigate whether any color attribute of the 14 test color shades was affected by repeatability error, the correlated coefficient was

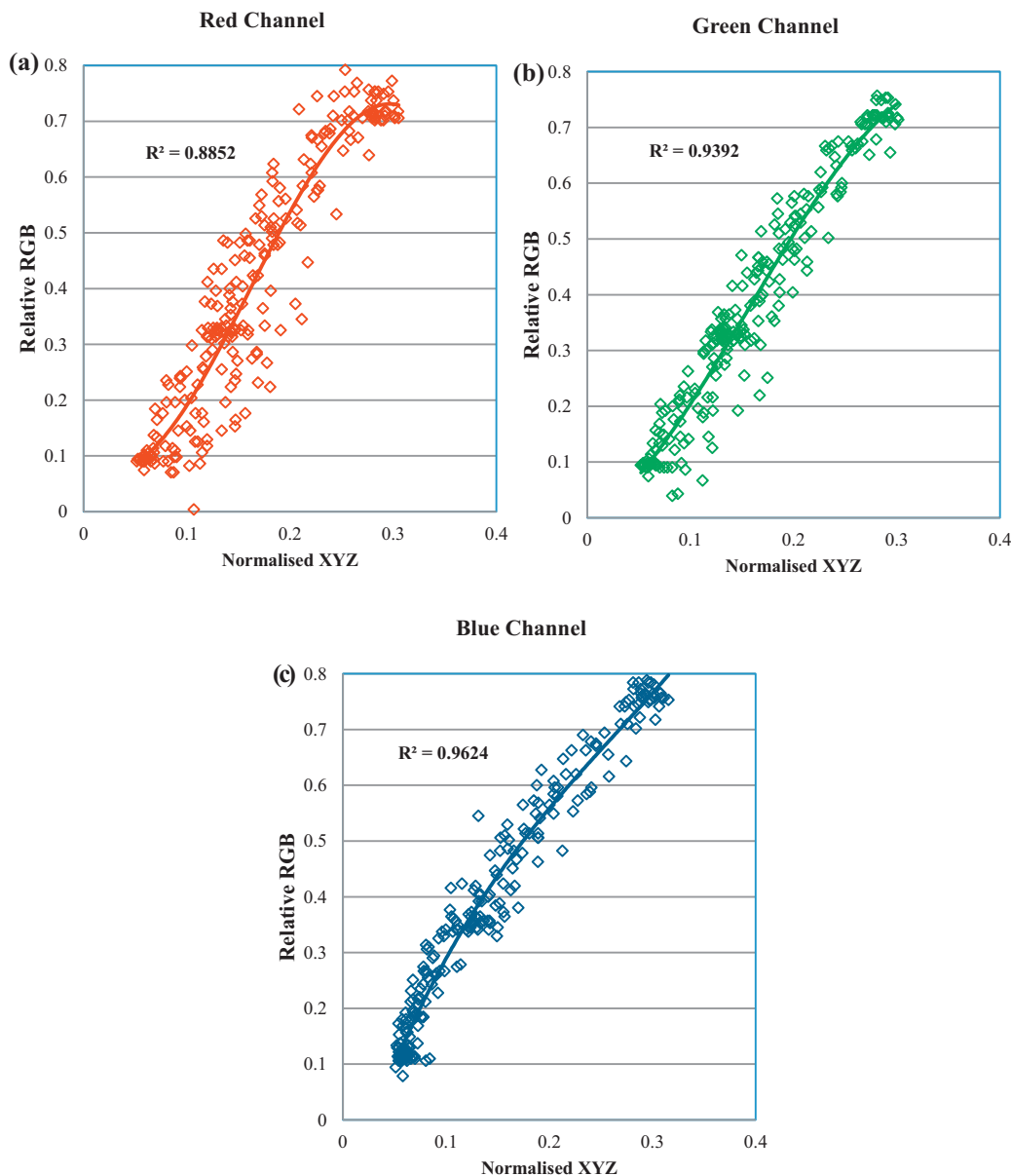


Fig. 3 – Relationship between normalised CIE XYZ Tristimulus values and corresponding relative printer RGB for Zcorp Z510 3D printer.

calculated for the relationship between each individual attribute (L^* , a^* or b^*) and the overall system error (represented by an average of 9 repeatability errors) for each test color, respectively. The results were 0.65, 0.03 and 0.85 for L^* , a^* and b^* , indicating that L^* and b^* could affect the repeatability error significantly.

Therefore, it is recommended that the color repeatability should be evaluated before any soft tissue prostheses are produced. In essence, if the repeatability error is above $5\Delta E_{ab}^*$, the color reproduction system will need to be calibrated using new color measurement data.

3.4. Performance of color gamut

The color gamut for the proposed 3D color printing system was simulated with the maximum and minimum color outputs in terms of lightness and chroma range evaluated. For this system the lightness (L^*) ranged from 29 to 74, which is comparatively low when compared to that of a normal color inkjet printer ($L^* - 0-96$). This indicates that, extremely dark

Table 2 – Color difference between original color chart and reproduction color charts.

Color reproduction	Mean	Max	Min	STDEV
CIE ΔE_{ab}^*	4.3	10.0	0.2	2.1

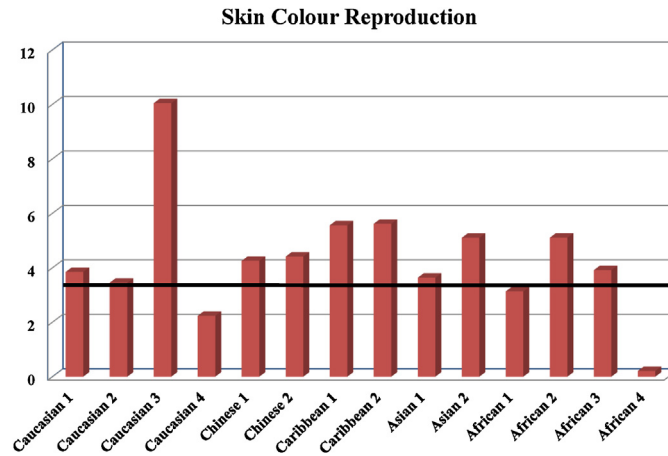


Fig. 4 – Color reproduction for human skin colors.

Table 3 – Performance of color repeatability test.

ΔE_{ab}^*	5 days	7 days	8 days	13 days	14 days	15 days	16 days	18 days	20 days
Color shade	3.1	3.5	2.7	1.9	2.5	3.5	2.7	2.3	5.0
Clear shade	2.4	3.3	1.4	0.2	1.5	0.9	1.0	1.6	3.1

and bright colors cannot be reproduced with the same accuracy when using the 3D printing system. This is primarily due to the color being printed within the starch powder rather than on glossy paper. The Chroma range for colors produced by the 3D printing system was between 0 and 85, indicating that high color intensity for the colors within the printer gamut can be achieved.

As detailed the main focus of this study was the accurate reproduction of human skin colors for the application of soft tissue prostheses produced by 3D printing. Fig. 6 illustrates the color gamut of the 3D printing system for the 14 skin colors adopted within the CIELAB uniform color space. Fig. 6a represents the top view chromaticity diagram on the

CIELAB uniform color space, whereas Fig. 6b represents the side view of the CIELAB uniform color space. The mesh lines represent the color gamut of the proposed 3D color printing system. 14 spheres were plotted to represent the distribution of the human skin test colors used. All colors within the mesh line were within the color gamut of the 3D printing system and therefore can be reproduced accurately.

It can also be seen that the vast majority of the skin colors are well within the printer color gamut apart from one color which is just outside. The only color found to be outside the color gamut of the printer was Caucasian 3. The evaluation thus demonstrates that most skin colors can be reproduced

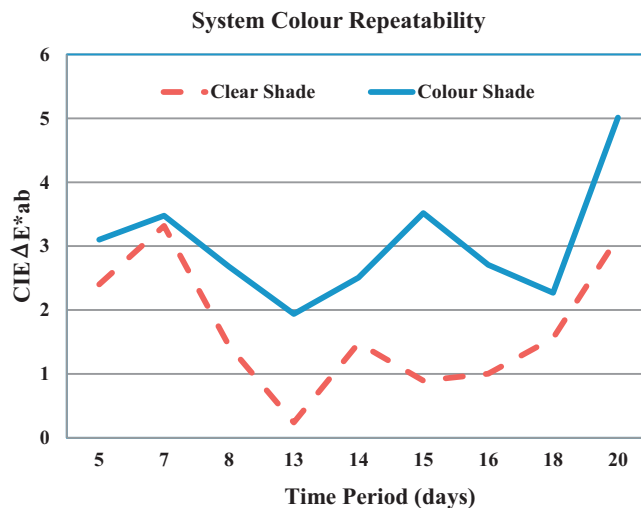


Fig. 5 – Performance of color repeatability for colors and clear shades.

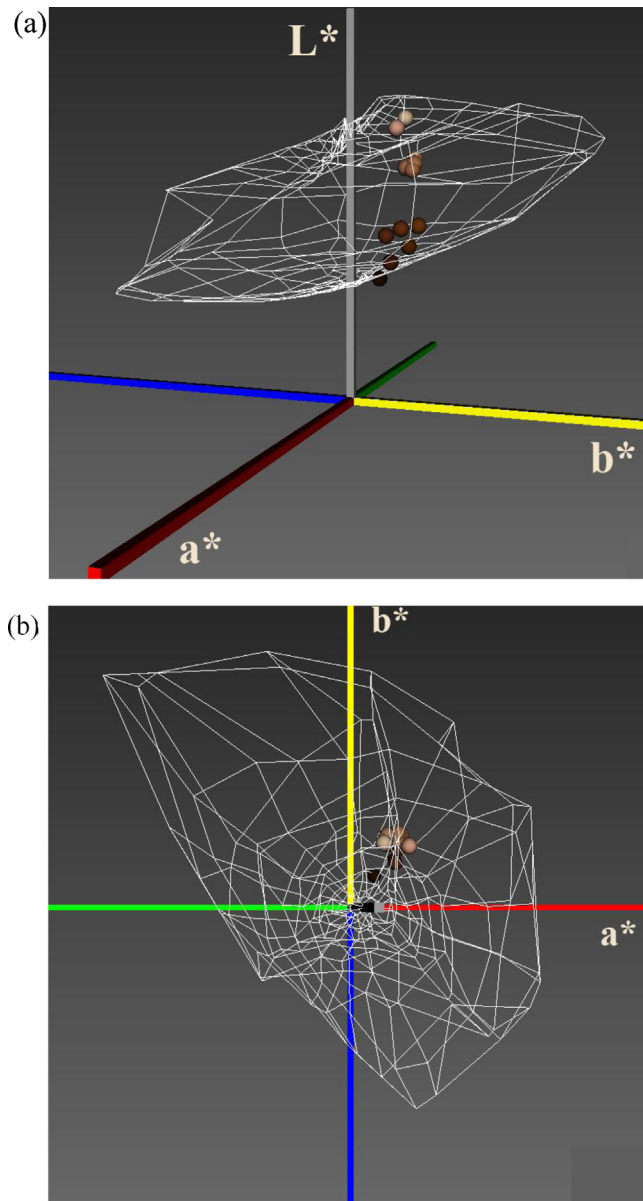


Fig. 6 – Color gamut of 3D printing system for 14 human skin colors: (a) top view and (b) side view.

using the proposed 3D printing system. However, some extremely dark or bright skin colors may fall just outside the color gamut of the printing system used and thus could not be reproduced accurately.

4. Conclusions

In this study, we proposed a color reproduction system for the advanced manufacture of soft tissue prostheses. A 3D printing system was adopted that printed 3D objects using a Zcorp Z510 3D color printer and silicone infiltrated starch powder models. Using a sample of 240 printed training colors, the color profile for the 3D color printing system was developed using a third order polynomial regression model. The color reproduction system was developed and system performance was then

evaluated using a sample of 14 known human skin colors. The average color reproduction error was approximately $4.3\Delta E_{ab}^*$. Taking into account the color repeatability error it was deemed that the color performance was acceptable. Furthermore, the color repeatability and color gamut for the 3D printing system were also evaluated. The results obtained led to the formulation of certain recommendations for use of this system for skin color reproduction.

Conflict of interest statement

There is no conflict of interest for all authors.

Acknowledgements

This study was partially supported by the Wellcome Trust Translational Research Award UK-Automated rapid manufacture of facial soft tissue prostheses and Fripp Design Limited, UK.

REFERENCES

- Leonardi A, Buonaccorsi S, Pellacchia V, Moricca LM, Indrizzi E, Fini G. Maxillofacial prosthetic rehabilitation using extraoral implants. *Journal of Craniofacial Surgery* 2008;19:398–405.
- Valauri AJ. Maxillofacial prosthetics. *Aesthetic Plastic Surgery* 1982;6:159–64.
- Beatty MW, Mahanna GK, Jia W. Ultraviolet radiation-induced color shifts occurring in oil-pigmented maxillo elastomers. *The Journal of Prosthetic Dentistry* 1999;82:441–6.
- Dimitrov D, Schreve K, de Beer N. Advances in three dimensional printing – state of the art and future perspectives. *Rapid Prototyping Journal* 2006;12:136–47.
- van Noort R. The future of dental devices is digital. *Dental Materials* 2011;28:3–12.
- van Noort R, Yates JM, Fripp T, Wildgoose D. Method for manufacturing a prosthesis using colour and geometrical data. World Patent WO2012123693 (A1); 2012.
- Johnson T. Colour management in graphic art and publication. Leatherhead: Pira International; 1996.
- CIE Technical Report, *Colorimetry*, 3rd ed. Publication 15. Vienna: CIE Central Bureau; 2004.
- Kang HR. Colour scanner calibration. *Journal of Imaging Science Technology* 1992;36:162–70.
- Kang HR, Anderson PG. Neural network applications to the colour scanner and printer calibration. *Journal of Electronic Imaging* 1992;1:125–34.
- Xiao K, Zardawi F, Yates JM. Colour management system for displaying microscope imaging. *Displays* 2012;33:214–20.
- Hong G, Luo MR, Rhodes PA. A study of digital camera colorimetric characterization based on polynomial modelling. *Color Research and Application* 2001;26:76–84.
- Johnson T. Methods for characterizing colour scanners and digital cameras. *Displays* 1996;16:183–91.
- Xiao K, Lao N, Zardawi F, Liu H, van Noort R, Yang Z, et al. An investigation of Chinese skin colour and appearance for skin colour reproduction. *Chinese Optics Letter* 2012;10:083301.

-
15. Morovič J, Luo MR. Calculating medium and image gamut boundaries for gamut mapping. *Color Research and Application* 2000;25:394–401.
 16. Bakke MA, Farup I, Hardeburg JY. Evaluation of algorithms for the determination of color gamut boundaries. *Journal of Imaging Science and Technology* 2010;54:50502–11.
 17. Paravina RD, Majkic G, Del Mar Perez M, Kiat-amnuay S. Color difference thresholds of Maxillo skin replications. *Journal of Prosthodontics* 2009;18:618–25.
 18. MacDonald LW, Morovic J, Xiao K. A topographic gamut compression algorithm. *Journal of Imaging Science and Technology* 2002;46:228–36.